Dyes and Pigments 94 (2012) 561–569

Contents lists available at SciVerse ScienceDirect

Dyes and Pigments

journal homepage: www.elsevier.com/locate/dyepig

Xanthene-based phosphine oxide host with the planar multi-insulating structure for efficient electrophosphorescence

Chunmiao Han [a], Guohua Xie [b], Hui Xu [a,*], Zhensong Zhang [b], Pengfei Yan [a], Yi Zhao [b,*], Shiyong Liu [b]

[a] Key Laboratory of Functional Inorganic Material Chemistry, Ministry of Education, Heilongjiang University, 74 Xuefu Road, Harbin 150080, PR China
[b] State Key Laboratory on Integrated Optoelectronics, College of Electronics Science and Engineering, Jilin University, 2699 Qianjin Street, Changchun 130012, PR China

ARTICLE INFO

Article history:
Received 6 January 2012
Received in revised form
6 March 2012
Accepted 13 March 2012
Available online 23 March 2012

Keywords:
Phosphine oxide
Electrophosphorescence
Configuration
Multi-insulating linkage
Host
Xanthene

ABSTRACT

A phosphine oxide (PO) host containing planar xanthene (**XantPO**) was chosen to investigate the influence of the structure of chromophores on the properties of the host. Owing to the multi-insulating linkages, the planar structure of **XantPO** also realizes high first triplet excited level (T_1) of 2.92 eV, and supports excellent morphological and thermal stability with the high temperature of glass transition (T_g, 135 °C) and temperature of decomposition (T_d, 369 °C). On the basis of theoretical simulation and electrochemical analysis and bright and efficient green and blue phosphorescent organic light-emitting diodes (PHOLEDs) of **XantPO**, it indicated that the configuration of chromophores in hosts can remarkably influence the device performance even if their optical properties were very approximate.

1. Introduction

In recent decades, phosphorescent organic light-emitting diodes (PHOLEDs) have attracted considerable attention owing to their nearly 100% internal quantum efficiency through harvesting both singlet and triplet excitons [1–5]. Due to the long lifetime of triplet excitons, phosphorescent materials generally exhibit serious triplet–triplet annihilation and triplet-polaron annihilation under electrical field [6,7]. To solve this problem, the phosphors are often dispersed in organic host matrixes. For the time being, the performance of green and red PHOLEDs based on doping/blending systems has approached to commercial requirements [8–14]. However, outstanding blue electrophosphorescent devices remains a greatly challenge due to the lack of appropriate host materials. In general, an ideal host should possess the characteristics as: (i) its first triplet excited level (T_1) must be higher than that of the dopants to prevent the reverse energy transfer from guest to host and reduce the non-radiative losses; (ii) it should have good carrier injecting/transporting properties to reduce the driving voltage and the efficiency roll-off; (iii) it should have excellent morphological, thermal and chemical stabilities to benefit the devices fabrication and improve the device lifetime. Therefore, a critical challenge in this field is to design and synthesis of efficient hosts which possess both high T_1 and excellent electrical properties. Unfortunately, these two factors are actually interrelated contradictories. It is believed that high triplet excited level requires the limited degree of molecular conjugation. But then, the wider and longer overlaps of p/π electron clouds profit the intra- and inter-molecular carrier injecting and transporting. How to solve this contradiction remains urgent and challenging. We always believe that figuring out the relationship between the molecular structures and the properties of the hosts can give valuable suggestions for this question.

With the aim to achieve efficient hosts with high T_1, some important strategies of structure design, such as meso, twisted and insulating linkage, are brought up for carbazole [6,8,12,13,15–27] and/or silane-based host materials [28,29]. However, the unipolar characteristics of carbazole and the electric inertia of saturated C and Si atoms result in the high driving voltages of their devices. Although some more complicated hosts based on carbazole and silane hybrid [30–33] were designed with the combination of advantages of good hole-transporting abilities and high T_1, the driving voltages of their devices remained above 5 V. In recent years, hosts based on phosphine oxide (PO) aroused great interest

* Corresponding authors. Tel.: +86 451 59886195; fax: +86 451 86608042.
E-mail addresses: hxu@hlju.edu.cn (H. Xu), zhao_yi@jlu.edu.cn (Y. Zhao).

0143-7208/$ – see front matter © 2012 Elsevier Ltd. All rights reserved.
doi:10.1016/j.dyepig.2012.03.013

since their prominent advantages as (i) the phosphine oxide (PO) moieties link the aromatic groups through saturated C–P bond, which blocks the conjugation extension and preserves their high triplet energy; (ii) it has been proved that PO moieties could effectively polarize molecules and enhance their electron injecting/transporting ability. That means that phosphine oxide-based host molecules could have both high T_1 and good carrier injecting/transporting ability. Many phosphine oxide host materials based on carbazole [34–40], fluorene [41–44], dibenzofuran [45–48] and spirofluorene [49,50] with high T_1 (approach to 3.0 eV) are achieved. The relationship between the molecular structures and the properties and EL performance are also investigated. Nevertheless, most of the studies are focused on the influences of the position and number of the substituents on the properties of the hosts. Our group reported several effective strategies of PO hosts involving short-axis, indirect or multi-insulating linkage [43,46,47,51,52]. The corresponding model hosts endowed their blue/white PHOLEDs with low operating voltage and excellent efficiency stability. It was showed that the substituting position and linkage mode can indeed tune the carrier injecting/transporting properties and the excited energy levels. Then, how the configurations of the chromophores influence the properties and performance of the hosts becomes an interesting question. It is known that the planar structure is superior in carrier injecting/transporting due to the more feasible inter-molecular stacking or overlap. Recently, we reported a simple PO host named bis(2-(diphenylphosphino)phenyl) ether oxides (**DPEPO**), whose structure is six individual phenyls linked through one oxygen atom and two P=O moieties, namely multi-insulating linkage [52]. Its structure is flexible since the system is formed through rotatable σ bonds, which seems inferior in carrier injecting/transporting. However, whether this can be an important constraint having remarkable effect on the device performance is still unclear.

In this paper, we chose another phosphine oxide host based on xanthene, 9,9-dimethyl-4,6-bis(diphenylphosphoryl)xanthene (**XantPO**, Scheme 1), which is formed by substitution of 9,9-Dimethylxanthene with two diphenyl phosphine oxide (DPPO) moieties. The six phenyls are also segregation by three kinds of insulating linkages. The intrinsic difference between **XantPO** and **DPEPO** is the former has a planar multi-insulating structure. Therefore, their optical properties may be similar. However, the planar structure can endow **XantPO** with improved thermal stability and the elevated highest occupied molecular orbital (HOMO). The bright and efficient green and blue electrophosphorescence based on **XantPO** was realized. The differences between the device performance of **XantPO** and **DPEPO** were also discussed in detail. It indicated that the configurations of chromophores can also influence the carrier injecting/transporting and consequently the voltage–current characteristics and efficiencies, which should also be taken into consideration when choosing chromophore moieties in PO hosts.

2. Experimental section

2.1. Materials and instruments

All the reagents and solvents used for the synthesis of the title compound were purchased from Aldrich and Acros companies and used without further purification.

^{1}H NMR spectra were recorded using a Varian Mercury plus 400NB spectrometer relative to tetramethylsilane (TMS) as internal standard. Absorption and PL emission spectra of the target compound were measured using an SHIMADZU UV-3150 spectrophotometer and an SHIMADZU RF-5301PC spectrophotometer, respectively. Thermogravimetric analysis (TGA) and differential scanning calorimetry (DSC) were performed on Shimadzu DSC-60A and DTG-60A thermal analyzers under nitrogen atmosphere at a heating rate of 10 °C min^{-1}. Phosphorescence spectra were measured in dichloromethane using an Edinburgh FPLS 920 fluorescence spectrophotometer at 77 K cooling by liquid nitrogen.

2.2. Synthesis

9,9-Dimethyl-4,6-bis(diphenylphosphoryl)xanthene (**XantPO**): At room temperature 4.36 ml of *n*-butyllithium (2.4 M in n-hexane, 10.47 mmol) was added dropwise to a stirred solution of 1.00 g of 9,9-dimethylxanthene (4.76 mmol) and 1.65 ml of N,N,N′,N′-tetramethylethenyldiamine (TMEDA) (10.47 mmol) in 50 ml of dry THF. After all *n*-butyllithium was added, the reaction mixture was stirred for 16 h. Then a solution of 2.06 ml of chlorodiphenylphosphine (10.47 mmol) in 10 ml of THF was added dropwise, and the reaction mixture was stirred for another 16 h. The reaction was quenched by 10 ml of water, and extracted by dichloromethane (3 × 30 ml). The organic layer was dried with anhydrous Na_2SO_4. The solvent was removed in *vacuo*. The residue was dissolved by 50 ml of dichloromethane. Then 3 ml of hydrogen peroxide (30%) was added, and the reaction mixture was stirred for 4 h. The mixture was washed with aqueous $NaHSO_3$ saturated solution and water successively. The organic layer was separated and dried with anhydrous Na_2SO_4. The solvent was removed in *vacuo*. The residue was purified through flash column chromatograph. Yield: 2.33 g of white powder (80%). ^{1}H NMR (400 MHz, $CDCl_3$, TMS): $\delta = 7.599$ (d, $J = 7.6$ Hz, 2 H), 7.486–7.370 ppm (m, 12 H), 7.358–7.261 ppm (m, 8 H), 6.981 (d, $J = 7.6$ Hz, 2 H), 6.780 (q, $J = 7.4$ Hz, 14.6 Hz, 2 H), 1.694 (s, 6 H). ESI-MS (*m*/*z*, %): 610 (M^+, 100); elemental analysis (%): for calculated C 76.71, H 5.28, O 7.86; found C 76.78, H 5.33, O 7.94.

2.3. Theoretical calculation

Computations on the electronic ground-state of the compounds were performed using Becke's three-parameter density functional in combination with the nonlocal correlation functional of Lee,

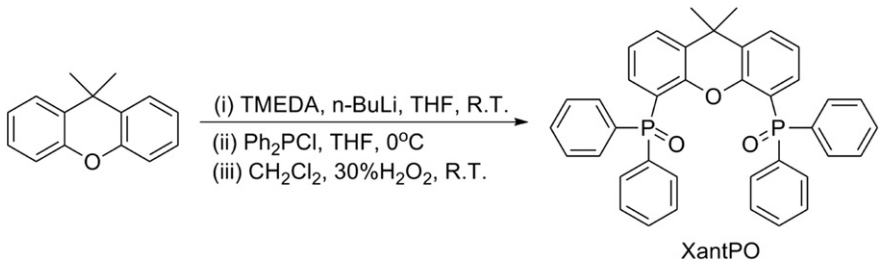

Scheme 1. Synthetic procedure for **XantPO**.

Yang, and Parr (B3LYP). 6-31G(d) basis sets were employed. The ground-state geometries were fully optimized at the B3LYP level. All computations were performed using the Gaussian 03 package.

2.4. Device fabrication

Prior to the device fabrication, the patterned ITO-coated glass substrates were scrubbed and sonicated consecutively with acetone, ethanol, and de-ionized water, respectively. All the organic layers were thermally deposited in vacuum ($\sim 4.0 \times 10^{-4}$ Pa) at a rate of 1–2 Å/s monitored in situ with the quartz oscillator. In order to reduce the ohmic loss, a heavily p-doped layer with MoO_x, considering the low doping efficiency in amorphous organic matrix with transition-metal-oxide-based acceptors, was directly deposited onto the ITO substrate for each sample. After the deposition of LiF, the samples were transferred to metal chamber, and suffered from a vacuum break due to the change of the shadow masks to determine the active area. The current-voltage luminance characteristics were measured with a PR650 spectrascan spectrometer and a Keithley 2400 programmable voltage–current source. All the samples were measured directly after fabrication without encapsulation in ambient atmosphere at room temperature.

3. Results and discussion

3.1. Design and synthesis

With the aim to investigate the influence of the configurations of chromophores on the properties of the corresponding PO hosts, any other functional linkages or modifications should be avoided. Since we chose **DPEPO** as the reference, the other PO host should have the similar substituents and functional groups. Thus, the planar structure of this PO compound should be formed without any supererogatory modifications. In this sense, **XantPO** is suitable since its planar structure is based on the linkage of biphenylether through an isopropylene. As the results, in **XantPO** the six phenyls are segregated through three insulating linkages as ether linkage, saturated carbon linkage and PO linkage. These individual phenyls are similar with those in **DPEPO**. The difference between **XantPO** and **DPEPO** is their different chromophores (xanthene in the former and diphenylether in the latter). Although xanthene is planar, the conjugation between its two phenyls is absolutely blocked by O atom and 9-saturated C atom. Therefore, the planar configuration of **XantPO** does not increase its conjugated length and area. This is the basis of our investigation. The DPPO moieties in **XantPO** were also substituted along the short-axis in order to reserve the high triplet level and enhance the polarizability of P=O bonds. The formation of planar structure may increase the molecular rigidity, which have effect on improving the thermal and morphological stability. Furthermore, the methyls on 9-C could facilitate the evaporation ability of the molecule and increase the inter-molecular hindrance to reduce the multi-particle annihilation (MPA).

XantPO was conveniently prepared through a three-step procedure of regioselective lithiation, phosphorization and oxidation, with good total yield over 80% (Scheme 1). The structure characterization was established on the basis of mass spectrometry, NMR spectroscopy and elemental analysis.

3.2. Thermal properties

Differential scanning calorimetry (DSC) and thermogravimetric analysis (TGA) were performed to investigate the thermal properties of **XantPO** (Fig. 1). The decomposition temperature (T_d, corresponding to 5% weight loss) of **XantPO** is as high as 386 °C, which is

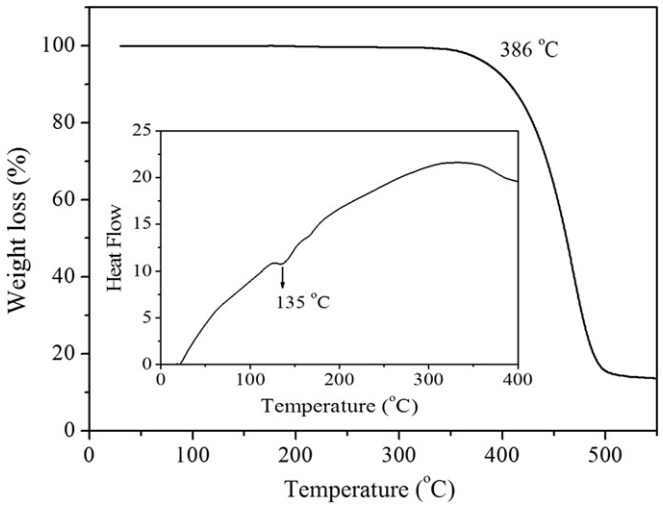

Fig. 1. TGA and DSC curves of **XantPO**.

increased for 64 °C compared with that of the **DPEPO** (322 °C) [52]. The remarkably improved T_d of **XantPO** can be obviously ascribed to the involvement of the planar and rigid xanthene. Significantly, the glass transition temperature (T_g) of **XantPO** is very high as 135 °C, which is 70 °C higher than that of mCP and is outstanding among the small molecular hosts. Furthermore, there is no endothermal peak corresponding to melting point (T_m) observed before **XantPO** decomposited. This implied either **XantPO** is reluctant to crystallize due to the combined steric effect of DPPOs and methyls, or T_m of **XantPO** should be more than 380 °C, which is at least 100 °C higher than that of **DPEPO** and can be attributed to the enhanced π-π inter-molecular interaction owing to the planar xanthene. Obviously, the planar structure of **XantPO** significantly improves the thermal performance. Simultaneously, the short-axis substitution of steric DPPO moieties further enhances the molecular rigidity of **XantPO**, which restrains the structure adjustment of the whole molecule and results in the high T_g. It indicated that the planar structure is superior in thermal and morphological stability, which can effectively suppress the potential Joule heat induced phase separation during device operating. This is very beneficial to achieve long device lifetime.

3.3. Optical properties

UV/vis and photoluminescent (PL) spectra of **XantPO** in dilute CH_2Cl_2 solutions (1×10^{-6} mol L^{-1}) and in film were measured to investigate its optical properties (Fig. 2). In solution, **XantPO** has three absorption bands at 287, 254 and 228 nm. The absorption bands at 287 and 254 nm can be attributed to $n \rightarrow \pi^*$ and $\pi \rightarrow \pi^*$ transitions of xanthene, respectively, while the band at 230 nm is originated from $\pi \rightarrow \pi^*$ transition of phenyls in DPPO moieties. It means that xanthene acts as the antenna of energy absorption in the molecule. Furthermore, in film, these three absorption bands only shift red for 2–6 nm, which indicates the reduced inter-molecular interaction and restrained aggregation owing to the enhanced steric effect of methyls and DPPO moieties. The emissions of **XantPO** in dilute solution and film are very similar with the peaks at 331 and 335 nm, respectively. This further demonstrated its weak aggregation in solid state. Meanwhile, PL emission peak of **XantPO** is ranged from 300 to 550 nm which is fully overlap with the metal to ligand charge transfer (MLCT) absorption peaks of the blue-emitting phosphor iridium(III)bis(4,6-(difluorophenyl) pyridinato-N,C2)picolinate (FIrpic) and green-emitting phosphor

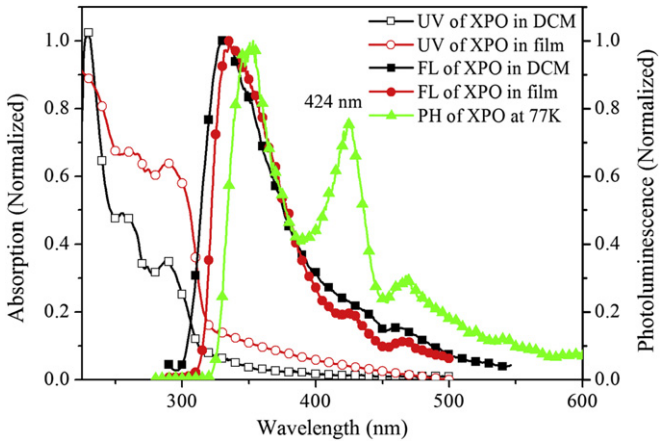

Fig. 2. UV/Vis and PL spectra of **XantPO**.

iridium(III)bis(2-phenylpyridinato-C2,N)acetylacetonate ($Ir(ppy)_2$acac). The lifetime of **XantPO** is as long as 1.79 ns. Therefore, the stable excited state can be expected, which is beneficial for energy transfer from host to guest. To determine T_1, the low temperature emission spectrum of **XantPO** in CH_2Cl_2 glass was also measured at 77 K, in which the first peak at 350 nm is attributed to fluorescent emission and the second peak at 424 nm is corresponding to the 0–0 transition of triplet emission. Therefore, T_1 level of **XantPO** can be estimated as 2.92 eV, which is higher than the common blue dopant FIrpic and green dopant $Ir(ppy)_2$acac. Therefore, its efficient energy transfer to these phosphors can be expected. It is noticed that the optical properties of **XantPO** and **DPEPO** are very similar, including emission peaks (308 nm for **DPEPO** and 321 nm for **XantPO**) and T_1 levels (2.99 eV for **DPEPO** and 2.92 eV for **XantPO**). This demonstrated that the multi-insulating linkage in **XantPO** efficiently restrained the influence of planar structure on the molecular electronic characteristics. Therefore, in the sense of photophysical properties, **DPEPO** and **XantPO** should be very approximate. Nevertheless, It is noticed that **DPEPO** has bigger optical energy gap of 4.05 eV than that of **XantPO** (3.91 eV).

3.4. DFT calculation

Frontier molecular orbitals (FMOs) of **XantPO** were investigated to understand the physical properties of **XantPO** at molecular level by the density functional theory (DFT) calculations (Fig. 3). The simulation result of **DPEPO** was also presented for comparsion. As shown in Fig. 3, the electron cloud distributions of HOMO and LUMO of **XantPO** are mainly localized in the xanthene moiety. This is diametrical to **DPEPO**, whose HOMO and LUMO are absolutely separated and contributed by diphenylether and DPPOs respectively. LUMO+1 and LUMO+2 of **XantPO** were contributed by both DPPOs and xanthene. The excessively centralized contributions of the simplex moiety to FMOs may induce the unbalanced carrier injecting/transporting, since one group commonly can not possess bipolar characteristics. The calculated LUMOs of **XantPO** and **DPEPO** are the same as −0.735 eV, while their calculated HOMOs are −5.823 and −6.258 eV, respectively (Fig. 3). Therefore, HOMO-LUMO energy gap (E_g) of **XantPO** is 5.088 eV, which is 0.435 eV smaller than that of **DPEPO**. This is in accord with the difference between their optical energy gaps (0.24 eV). It is noticed that the planar structure of **XantPO** has more contribution in facilitating the hole injecting.

3.5. Electrochemical properties

The redox behaviors of **XantPO** and **DPEPO** were investigated by cyclic voltammetry (CV) at room temperature in CH_2Cl_2 measured against an Ag/AgCl (0.1 M) electrode (Fig. 4). Both of these two compounds displayed irreversible one-electron oxidation waves at 2.25 and 2.68 V, respectively. Their onset potentials were 1.81 and 1.93 V, respectively. According to the equation $E_{HOMO} = (E^{Oxy}_{onset} + 4.4\ eV)$, E_{HOMO} of **XantPO** and **DPEPO** are about −6.21 and −6.33 eV, respectively. It is obvious that the planar

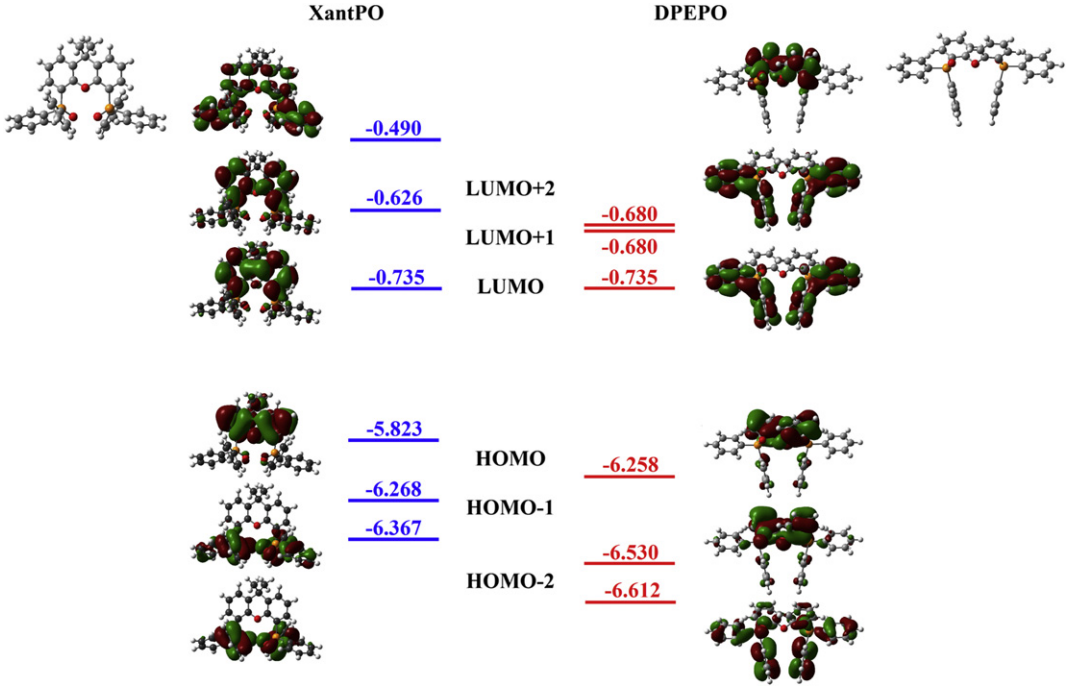

Fig. 3. DFT calculation results of **XantPO**.

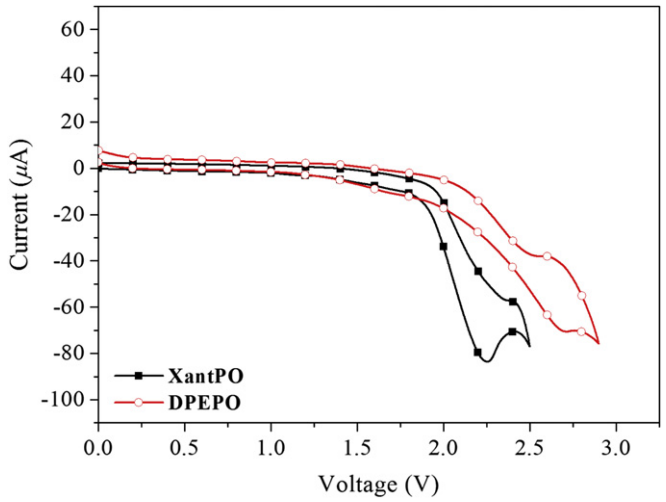

Fig. 4. CV curves of **XantPO** and **DPEPO**.

configuration of xanthene ring endows XantPO with higher HOMO to provide stronger hole injecting ability, which are in accordance with DFT calculation. Their LUMOs are −2.39 and −2.29 eV calculated by the optical energy gaps. The electrochemical analysis indicated that the planar xanthene can facilitate carrier injecting in **XantPO** compared with the flexible diphenylether in **DPEPO**.

3.6. EL properties

To investigate the performance of **XantPO** as hosts for green electrophosphorescence, Device **A** and **B** were fabricated with the configuration of ITO/MoO_x (2 nm)/4,4′,4′′-tri(*N*-3-methylphenyl-*N*-phenylamino)triphenylamine (*m*-MTDATA):MoO_x (15 wt.%, 30 nm)/*m*-MTDATA (10 nm)/Tris(phenylpyrazole)iridium (Ir(ppz)$_3$) (10 nm)/Ir(ppy)$_2$acac:**XantPO** (6%, *x* nm)/4,7-diphenyl-1,10-phenanthroline (BPhen) (50-*x* nm)/LiF (1 nm)/Al (*x* = 10 nm for **A** and 20 nm for **B**) were fabricated (Scheme 2), where MoO_x and LiF served as hole- and electron injecting layers, *m*-MTDATA and BPhen served as hole- and electron-transporting layers (HTL and ETL), Ir(ppz)$_3$ was used as hole-transporting and electron-blocking material, respectively. As shown in Fig. 5, Device **A** and **B** had low turn-on voltages of 3.0 and 3.5 V. The practical luminance of 100 and 1000 cd m^{-2} was achieved at the driving voltages of 3.5 and 4.1 V for **A** and 3.6 and 4.8 V for **B**, respectively. The lower driving voltages may be attributed to the reduced hole-injection barrier between hole-transporting layers (HTLs) and emitting layers (EMLs). Along with increasing the thickness of EML, the driving voltages also gradually increased, which implied that the electron injecting/transporting ability of **XantPO** is weaker than that of BPhen.

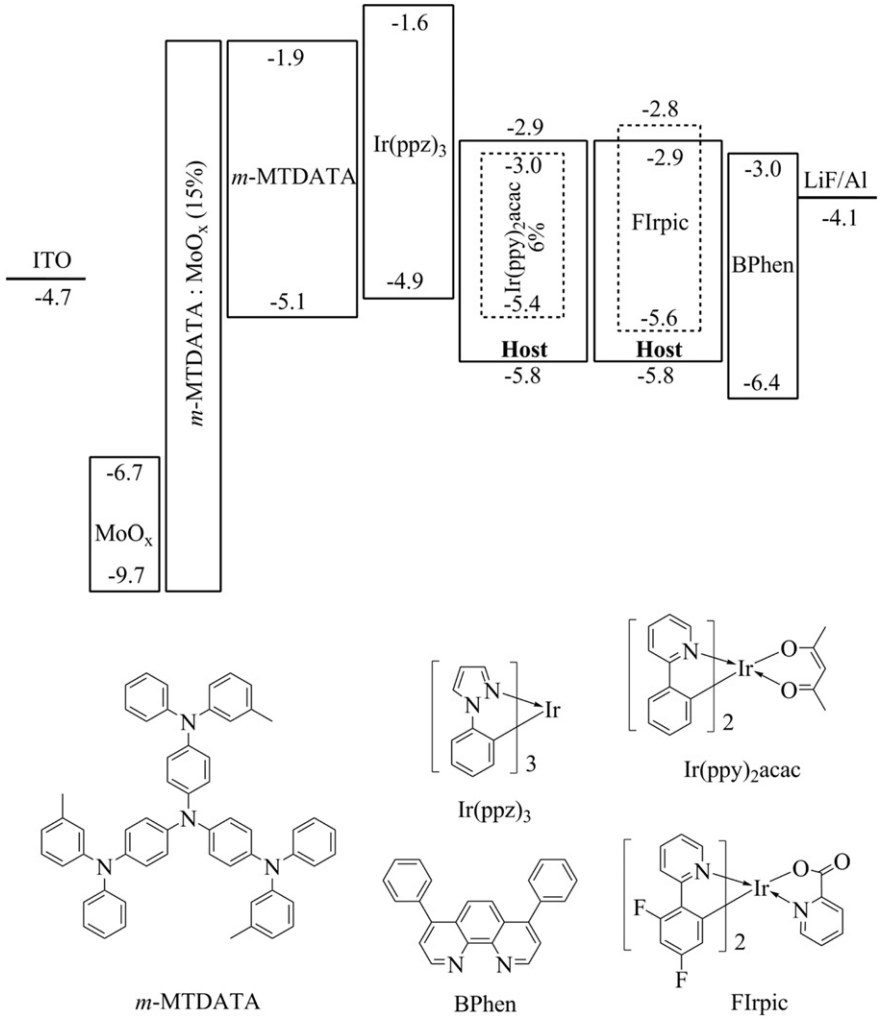

Scheme 2. Molecular structures and energy level diagram of the devices.

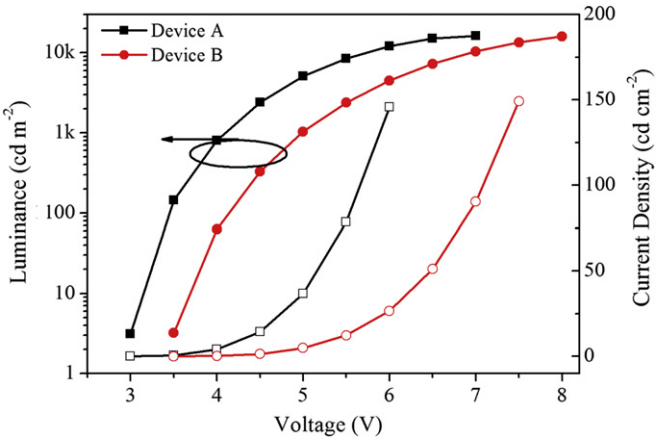

Fig. 5. Luminace-Current density–voltage curves of device **A** and **B**.

The maximum current efficiencies (C.E.) of **A** and **B** were 22.2 cd A^{-1} and 22.1 cd A^{-1} achieved at the luminance of 143.8 and 329 cd m^{-2} (Fig. 6). At the luminance of 1000 cd m^{-2}, C.E. of **A** and **B** were remained as 19.0 cd A^{-1} and 21.2 cd A^{-1}, respectively. The corresponding efficiency roll-offs were 14.4% and 4.1%. The maximum power efficiencies (P.E.) of **A** and **B** were achieved as 19.9 and 15.4 lm W^{-1} at the same luminance, and their P.E. were still 14.7 and 13.3 lm W^{-1} at the luminance of 1000 cd m^{-2}. The corresponding roll-offs were 26.1% and 13.6%. Furthermore, their maximum external quantum efficiencies (E.Q.E.) were the same as 6.2% (Fig. 6). The E.Q.E. roll-offs at 1000 cd m^{-2} were 14.5% and 4.8%, respectively. Therefore, Device **A** and **B** exhibited high and stable efficiencies. Although Device **A** had the lower driving voltages owing to its thinner EML and the consequential higher P.E., it is noticed that Device **B** exhibited much stable efficiencies and its C.E. and E.Q.E. at luminance more than 300 cd m^{-2} were even higher than those of **A**. This is in accord with the common view that a wider emission zone would increase the rate of radiative recombination and suppress the concentration quenching.

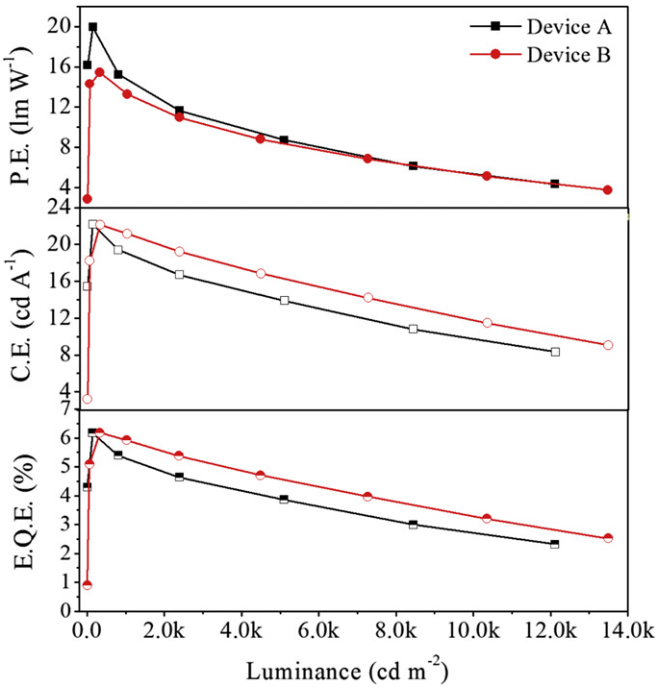

Fig. 6. Efficiency curves of device **A** and **B**.

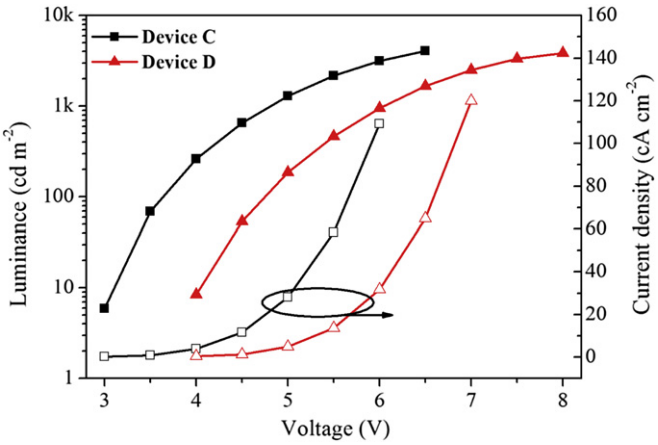

Fig. 7. Luminace–current density–voltage curves of device **C** and **D**.

The blue-emitting PHOLEDs based on **XantPO**, Device **C** and **D**, were fabricated with the same configurations except for the different dopant of FIrpic with the concentration of 10% (Scheme 2). The thickness of each layer of **C** and **D** was similar with that of **A** and **B**, respectively. Device **C** and **D** also had the low turn-on voltage of 3 V and 4 V (Fig. 7). The luminance about 1000 cd m^{-2} was achieved at 5.0 V for **C** and 6.0 V for **D**, respectively. Fig. 8 showed the efficiency-luminance curves of Device **C** and **D**, the maximum C.E. and P.E. of **C** and **D** were 7.47 and 4.08 cd A^{-1}, and 6.69 and 2.84 lm W^{-1}, respectively, corresponding to the maximum E.Q.E. of 4.03 and 2.21%, respectively. These data were moderate and worse than those of the best ambipolar and unipolar hosts reported before, which are more than 10% for E.Q.E. [53–56]. It is also noticeable that the performance of **XantPO** as host for blue electrophosphorescence was much worse than that of **DPEPO**, especially for efficiencies, although Device **C** and **D** exhibited more

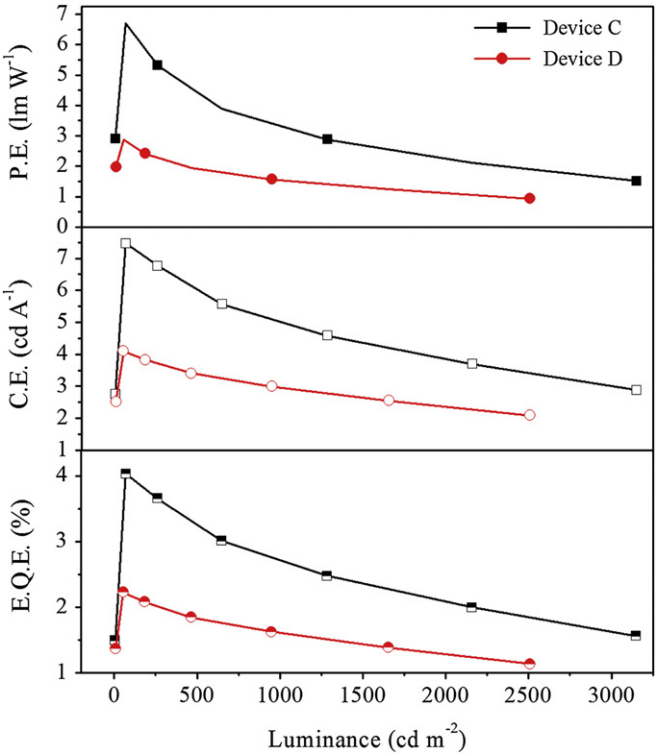

Fig. 8. Efficiency curves of device **C** and **D**.

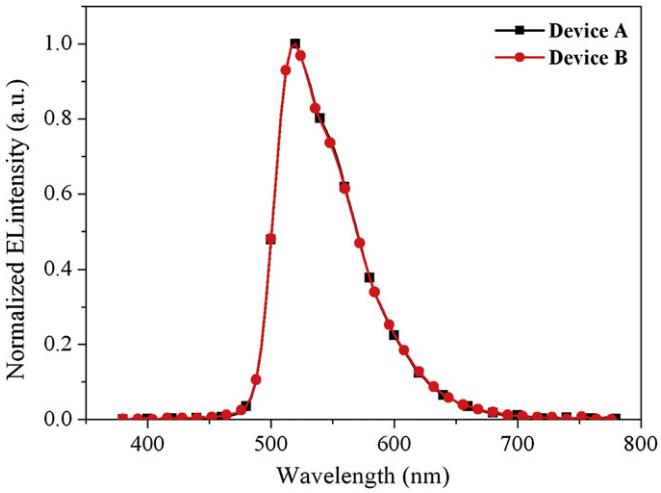

Fig. 9. EL spectra of device **A** and **B** at the biggest luminance.

stable efficiencies with reduced roll-offs: at 100 cd m^{-2}, 6.0% and 10.3% for P.E., 2.3% and 2.9% for C.E. and 2.7% and 3.6% for E.Q.E., respectively; at 1000 cd m^{-2}, 50.7% and 48.3% for P.E., 35.6% and 28.9% for C.E. and 34.0% and 28.8% for E.Q.E., respectively. Since the optical properties of **DPEPO** and **XantPO** are approximate, the main reason might be the unbalanced carrier injecting/transporting in **XantPO** compared with **DPEPO**. The planar structure of **XantPO** may also worsen the non-radiative transitions. The lower efficiencies of Device **D** can indicate the remarkable influence of carrier injecting/transporting in EML on device efficiencies. The small efficiency roll-offs of **XantPO**-based devices can be attributed to its rigid structure and improved thermal and morphological stability.

All of these four devices presented very stable EL spectra (Figs. 9 and 10). The intensities of the vibration bonds at long wavelengths were limited due to the effective localization of emission zones in EMLs, which improved the emission color purity as estimated by their Commission Internationale deL'Eclairage (CIE) coordinates shown in Table 1.

EL investigation indicated that only small variation of the molecular structure can remarkably influence the device performance even if the optical properties of the hosts were very approximate. The carrier injecting/transporting properties can be

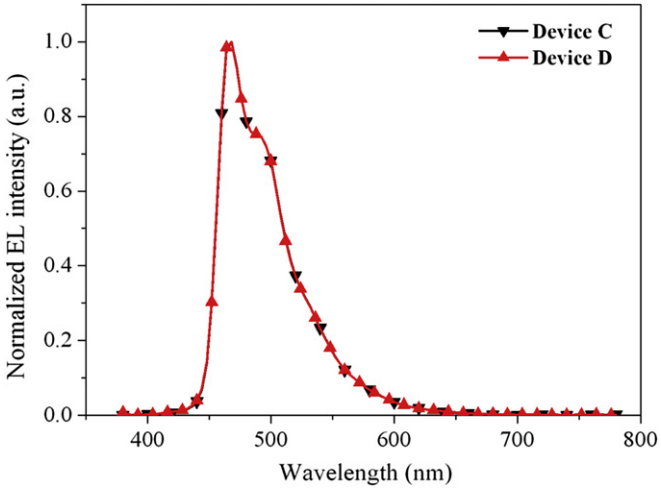

Fig. 10. EL spectra of device **C** and **D** at the biggest luminance.

Table 1
EL properties of device **A** ~ **D**.

Device	Driving voltage (V)	Max. efficiency[a]	Efficiency roll-off (%)[a]	CIE (*x*, y)
A	3.0,[b] 3.4,[c] 4.1[d]	22.1,22.2, 6.2	4.0,14.4, 14[d] 46.6,55.9, 56.2[e]	0.314, 0.624
B	3.5,[b] 3.6,[c] 4.8[d]	15.4,19.9, 6.2	13.6,25.6, 4.2[d] 65.1,73.0, 46.4[e]	0.314, 0.620
C	3.0[b], 4.1,[c] 5.0[d]	4.1, 7.5, 4.0	2.0, 1.6, 1.7[c] 27.4, 32.8, 32.8[d]	0.314, 0.280
D	4.0,[b] 4.7,[c] 6.0[d]	2.8, 6.7, 2.2	5.0,3.4, 1.8[c] 45.8,50.2, 27.6[d]	0.155, 0.278

[a] In the order of P.E. (lm/W), C.E. (cd/A) and EQE (%).
[b] Onset voltage.
[c] At 100 cd/m^2.
[d] At 1,000 cd/m^2.
[e] At 10,000 cd/m^2.

also influenced by the chromophore configurations and seemed the important restraints of the efficiencies. The casual changing of the molecular configuration would induce the unbalanced carrier injecting/transporting in EMLs and consequently reduce the efficiencies.

4. Conclusion

In summary, we chose a PO host containing planar xanthene (XantPO) on the basis of insulating linkages to investigate the influence of the structure of chromophores on the properties of the hosts through making comparison with its counterpart DPEPO. Owing to the multi-insulating linkages, the planar structure of XantPO does not influence its optical properties, which are nearly the same with those of DPEPO. Nevertheless, the planar structure endows XantPO with improved thermal and morphological stability and the elevated HOMO. The former has effect on reducing the efficiency roll-offs and might increase the device stability, while the latter would change the carrier injecting/transporting balance in EMLs. As the results, the bright and efficient green and blue PHOLEDs based on XantPO were demonstrated. The efficiency stability of the blue-emitting devices of XantPO was improved, although its maximum efficiencies were much less than those of DPEPO. It was showed that the configuration of chromophores in hosts can remarkably influence the device performance even if their optical properties were very approximate. The carrier injecting/transporting properties of the hosts seemed an important restraint of the efficiencies. The casual changing of the molecular energy levels and carrier mobility would induce the unbalanced carrier injecting/transporting in EMLs and consequently reduce the efficiencies. Therefore, more detailed tuning of the properties of the hosts, including the variation of the number and the position of the functional groups, should be essential for seeking for the efficient hosts, which is ongoing in our lab.

Acknowledgments

C.H. and G.X. contributed equally to this work. This work was financially supported by the National Key Basic Research and Development Program of China under Grant No. 2010CB327701, NSFC under Grant 50903028, 61176020 and 60977024, Key Project of Ministry of Education under Grant 212039, Supporting Programme of Heilongjiang Universities New Century Talents under Grant 1252-NCET-005, Education Bureau of Heilongjiang Province under Grant 2010td03, and Heilongjiang University under Grant 2010hdtd-08. CH thanks the supporting of Student Innovation Funds of Heilongjiang Province.

References

[1] Tsvetkov EN, Bondarenko NA, Malakhova IG, Kabachnik MI. A simple synthesis and some synthetic applications of substituted phosphide and phosphinite anions. Synthesis; 1986:198–208.

[2] Baldo MA, O'Brien DF, You Y, Shoustikov A, Sibley S, Thompson ME, et al. Highly efficient phosphorescent emission from organic electroluminescent device. Nature 1998;395:151–4.

[3] Lamansky S, Djurovich P, Murphy D, Abdel-Razzaq F, Lee H-E, Adachi C, et al. Highly phosphorescent bis-cyclometalated iridium complexes: synthesis, photophysical characterization, and Use in organic light emitting diodes. Journal of the American Chemical Society 2001;123:4304–12.

[4] Baldo MA, Thompson ME, Forrest SR. High-efficiency fluorescent organic light-emitting devices using a phosphorescent sensitizer. Nature 2000;403: 750–3.

[5] Reineke S, Lindner F, Schwartz G, Seidler N, Walzer K, Lussem B, et al. White organic light-emitting diodes with fluorescent tube efficiency. Nature 2009; 459:234–8.

[6] Baldo MA, Lamansky S, Burrows PE, Thompson ME, Forrest SR. [CBP] Very high-efficiency green organic light-emitting devices based on electrophosphorescence. Applied Physics Letters 1999;75:4–6.

[7] Baldo MA, Adachi C, Forrest SR. Transient analysis of organic electrophosphorescence. II. Transient analysis of triplet-triplet annihilation. Physical Review B 2000;62:10967.

[8] Tao YT, Wang Q, Yang CL, Wang Q, Zhang ZQ, Zou TT, et al. A simple carbazole/oxadiazole hybrid molecule: an excellent bipolar host for green and red phosphorescent OLEDs. Angewandte Chemie International Edition 2008;47: 8104–7.

[9] Chien C-H, Hsu F-M, Shu C-F, Chi Y. Efficient red electrophosphorescence from a fluorene-based bipolar host material. Organic Electronics 2009;10:871–6.

[10] Tao Y, Wang Q, Ao L, Zhong C, Yang C, Qin J, et al. Highly efficient phosphorescent organic light-emitting diodes hosted by 1,2,4-triazole-cored triphenylamine derivatives: relationship between structure and optoelectronic properties. The Journal of Physical Chemistry C 2009;114:601–9.

[11] Su SJ, Cai C, Kido J. RGB phosphorescent organic light-emitting diodes by using host materials with heterocyclic cores: effect of nitrogen atom orientations. Chemistry of Materials 2011;23:274–84.

[12] Lin M-S, Chi L-C, Chang H-W, Huang Y-H, Tien K-C, Chen C-C, et al. A diarylborane-substituted carbazole as a universal bipolar host material for highly efficient electrophosphorescence devices. Journal of Materials Chemistry; 2012.

[13] Yin C-R, Ye S-H, Zhao J, Yi M-D, Xie L-H, Lin Z-Q, et al. Hindrance-functionalized π-Stacked polymer host materials of the cardo-type carbazole–-fluorene hybrid for solution-processable blue electrophosphorescent devices. Macromolecules 2011;44:4589–95.

[14] Fan C-H, Sun P, Su T-H, Cheng C-H. Host and dopant materials for idealized deep-red organic electrophosphorescence devices. Advanced Materials 2011; 23:2981–5.

[15] Kawamura Y, Yanagida S, Forrest SR. [PVK] Energy transfer in polymer electrophosphorescent light emitting devices with single and multiple doped luminescent layers. J. Appl. Phys. 2002;92:87–93.

[16] Holmes RJ, Forrest SR, Tung Y-J, Kwong RC, Brown JJ, Garon S, et al. [mCP] Blue organic electrophosphorescence using exothermic host-guest energy transfer. Appl. Phys. Lett. 2003;82:2422–4.

[17] Tokito S, Iijima T, Suzuri Y, Kita H, Tsuzuki T, Sato F. [CDBP] Confinement of triplet energy on phosphorescent molecules for highly-efficient organic blue-light-emitting devices. Appl. Phys. Lett. 2003;83:569–71.

[18] Brunner K, van Dijken A, Börner H, Bastiaansen JJAM, Kiggen NMM, Langeveld BMW. Carbazole compounds as host materials for triplet emitters in organic light-emitting diodes: tuning the HOMO level without influencing the triplet energy in small molecules. Journal of the American Chemical Society 2004;126:6035–42.

[19] van Dijken A, Bastiaansen JJAM, Kiggen NMM, Langeveld BMW, Rothe C, Monkman A, et al. Carbazole compounds as host materials for triplet Emitters in organic light-emitting Diodes: polymer hosts for high-efficiency light-emitting diodes. Journal of the American Chemical Society 2004;126: 7718–27.

[20] Zhang Q, Chen J, Cheng Y, Wang L, Ma D, Jing X, et al. Novel hole-transporting materials based on 1,4-bis(carbazolyl)benzene for organic light-emitting devices. Journal of Materials Chemistry 2004;14:895–900.

[21] Shih P-I, Chiang C-L, Dixit AK, Chen C-K, Yuan M-C, Lee R-Y, et al. Novel carbazole/fluorene hybrids: host materials for blue phosphorescent OLEDs. Organic Letters 2006;8:2799–802.

[22] Chen H-F, Yang S-J, Tsai Z-H, Hung W-Y, Wang T-C, Wong K- T. 1,3,5-Triazine derivatives as new electron transport-type host materials for highly efficient green phosphorescent OLEDs. Journal of Materials Chemistry 2009;19: 8112–8.

[23] He J, Liu H, Dai Y, Ou X, Wang J, Tao S, et al. Nonconjugated carbazoles: a SERIES of novel host materials for highly efficient blue electrophosphorescent OLEDs. The Journal of Physical Chemistry C 2009;113: 6761–7.

[24] Sasabe H, Pu Y-J, Nakayama K, Kido J. m-Terphenyl-modified carbazole host material for highly efficient blue and green PHOLEDS. Chem. Commun; 2009:6655–7.

[25] Ye S, Liu Y, Chen J, Lu K, Wu W, Du C, et al. Solution-processed solid solution of a Novel carbazole Derivative for high-performance blue phosphorescent organic light-emitting diodes. Advanced Materials 2010;22:4167–71.

[26] An Z-F, Chen R-F, Yin J, Xie G-H, Shi H-F, Tsuboi T, et al. Conjugated Asymmetric Donor-substituted 1,3,5-Triazines: new host materials for blue phosphorescent organic light-emitting diodes. Chemistry – A European Journal 2011;17:10871–8.

[27] Zhang Y, Zuniga C, Kim S-J, Cai D, Barlow S, Salman S, et al. Polymers with carbazole-Oxadiazole Side Chains as ambipolar hosts for phosphorescent light-emitting diodes. Chemistry of Materials 2011;23:4002–15.

[28] Holmes RJ, D'Andrade BW, Forrest SR, Ren X, Li J, Thompson ME. [UGH1-2] Efficient, deep-blue organic electrophosphorescence by guest charge trapping. Appl. Phys. Lett. 2003;83:3818–20.

[29] Ren X, Li J, Holmes RJ, Djurovich PI, Forrest SR, Thompson ME. [UGH1-4] Ultrahigh energy gap hosts in deep blue organic electrophosphorescent devices. Chem. Mater 2004;16:4743–7.

[30] Tsai M-H, Lin H-W, Su H-C, Ke T-H, Wu C-C, Fang F-C, et al. Highly efficient organic blue electrophosphorescent devices based on 3,6-bis(triphenylsilyl) carbazole as the host material. Adv. Mater 2006;18:1216–20.

[31] Han W-S, Son H-J, Wee K-R, Min K-T, Kwon S, Suh I-H, et al. Silicon-Based blue Phosphorescence host materials: structure and photophysical Property relationship on Methyl/Phenylsilanes Adorned with 4-(N-Carbazolyl)phenyl groups and Optimization of their electroluminescence by Peripheral 4-(N-Carbazolyl)phenyl Numbers. The Journal of Physical Chemistry C 2009;113: 19686–93.

[32] Hu D, Lu P, Wang C, Liu H, Wang H, Wang Z, et al. Silane coupling dicarbazoles with high triplet energy as host materials for highly efficient blue phosphorescent devices. Journal of Materials Chemistry 2009;19: 6143–8.

[33] Gong S, Fu Q, Wang Q, Yang C, Zhong C, Qin J, et al. Highly efficient deep-blue electrophosphorescence enabled by solution-Processed bipolar tetraarylsilane host with both a high triplet energy and a high-Lying HOMO level. Advanced Materials 2011;23:4956–9.

[34] Sapochak LS, Padmaperuma AB, Vecchi PA, Qiao H, Burrows PE. Design strategies for achieving high triplet energy electron transporting host materials for blue electrophosphorescence. Proc. of SPIE 2006;6333:63330F.

[35] Sapochak L, Padmaperuma AB, Vecchi PA, Cai X, Burrows PE. Designing organic phosphine oxide host materials using heteroarmatic building blocks: inductive effects on electroluminescence. Proc. SPIE 2007;6655: 665506.

[36] Jeon SO, Lee JY. Synthesis of fused phenylcarbazole phosphine oxide based high triplet energy host materials. Tetrahedron 2010;66:7295–301.

[37] Jeon SO, Son HS, Yook KS, Lee JY. Ethylcarbazole based phosphine oxide derivatives as hosts for blue phosphorescent organic light-emitting diodes. Mol. Cryst. Liq. Cryst 2010;530:123/[279]–130/[286].

[38] Jeon SO, Yook KS, Joo CW, Lee JY. High-efficiency deep-blue-Phosphorescent organic light-emitting diodes using a phosphine oxide and a phosphine sulfide high-triplet-energy host material with bipolar charge-transport properties. Adv. Mater 2010;22:1–5.

[39] Jeon SO, Jang SE, Son HS, Lee JY. External quantum efficiency above 20% in deep blue phosphorescent organic light-emitting diodes. Adv. Mater 2011;23: 1436–41.

[40] Sapochak LS, Padmaperuma AB, Cai X, Male JL, Burrows PE. Inductive effects of diphenylphosphoryl moieties on carbazole host materials: design rules for blue electrophosphorescent organic light-emitting devices. J.Phys.Chem.C 2008;112:7989–96.

[41] Hsu F-M, Chien C-H, Shih P-I, Shu C-F. Phosphine-oxide-containing bipolar host material for blue electrophosphorescent devices. Chem. Mater 2009;21: 1017–22.

[42] Hsu F-M, Chien C-H, Shu C-F, Lai C-H, Hsieh C-C, Wang K-W, et al. A bipolar host material containing triphenylamine and diphenylphosphoryl-substituted fluorene units for highly efficient blue electrophosphorescence. Adv. Funct. Mater 2009;19:2834–43.

[43] Yu D, Zhao Y, Xu H, Han C, Ma D, Deng Z, et al. Fluorene-based phosphine oxide host materials for blue electrophosphorescence: an effective Strategy for a high triplet energy level. Chem. Eur. J 2011;17:2592–6.

[44] Yu D, Zhao F, Han C, Xu H, Li J, Zhang Z, et al. Ternary ambipolar phosphine oxide hosts based on indirect linkage for highly efficient blue electrophosphorescence: towards high triplet energy, low driving voltage and stable efficiencies. Adv. Mater 2012;24:509–14.

[45] Vecchi PA, Padmaperuma AB, Qiao H, Sapochak LS, Burrows PE. A dibenzofuran-based host material for blue electrophosphorescence. Org. Lett. 2006;8:4211–4.

[46] Han C, Xie G, Li J, Zhang Z, Xu H, Deng Z, et al. A new phosphine oxide host based on ortho-disubstituted dibenzofuran for efficient electrophosphorescence: towards high triplet state excited levels and excellent thermal, morphological and efficiency stability. Chemistry – A European Journal 2011;17:8947–56.

[47] Han C, Xie G, Xu H, Zhang Z, Yu D, Zhao Y, et al. Towards highly efficient blue-phosphorescent organic light-emitting diodes with low operating voltage and excellent efficiency stability. Chem. Eur. J 2011;17:445–9.

[48] Jeong SH, Seo CW, Lee JY, Cho NS, Kim JK, Yang JH. Comparison of bipolar hosts and mixed-hosts as host structures for deep-blue phosphorescent organic light emitting diodes. Chemistry – An Asian Journal 2011;6:2895–8.

[49] Lee J, Lee J-I, Lee JY, Chu HY. Improved performance of blue phosphorescent organic light emitting diodes with a mixed host system. Appl. Phys. Lett. 2009;95:253304.
[50] Zhao J, Xie G-H, Yin C-R, Xie L-H, Han C-M, Chen R-F, et al. Harmonizing triplet level and ambipolar characteristics of wide-gap phosphine oxide hosts toward highly efficient and low driving voltage blue and green PHOLEDs: an effective Strategy based on Spiro-Systems. Chemistry of Materials 2011;23:5331–9.
[51] Han C, Xie G, Xu H, Zhang Z, Xie L, Zhao Y, et al. A single phosphine oxide host for high-efficiency white organic light-emitting diodes with extremely low operating voltages and reduced efficiency roll-off. Advanced Materials 2011; 23:2491–6.
[52] Han C, Zhao Y, Xu H, Chen J, Deng Z, Ma D, et al. A simple phosphine–Oxide host with a multi-insulating structure: high triplet energy level for efficient blue electrophosphorescence. Chemistry – A European Journal 2011;17: 5800–3.
[53] Tao Y, Yang C, Qin J. Organic host materials for phosphorescent organic light-emitting diodes. Chemical Society Reviews 2011;40:2943–70.
[54] Lengvinaite S, Grazulevicius JV, Grigalevicius S, Lai YM, Wang WB, Jou JH. Polyethers containing 2-phenylindol-1-yl moieties as host materials for light emitting diodes. Synthetic Metals 2010;160:1793–6.
[55] Jou J-H, Wang W-B, Shen S-M, Kumar S, Lai IM, Shyue J-J, et al. Highly efficient blue organic light-emitting diode with an oligomeric host having high triplet-energy and high electron mobility. Journal of Materials Chemistry 2011;21: 9546–52.
[56] Zostautiene R, Grazulevicius JV, Lai YM, Wang WB, Jou JH, Grigalevicius S. Diphenylsilanes containing electronically isolated carbazolyl fragments as host materials for light emitting diodes. Synthetic Metals 2011;161:92–5.